Accepted Manuscript

Development of an optical biosensor for the detection of Trypanosoma evansi and Plasmodium berghei

Hay Thi Theint, James Edward Walsh, Wong Siew Tung, Kenny Voon Gah Leong, Mahendran Shitan

PII:	S1386-1425(19)30383-X
DOI:	https://doi.org/10.1016/j.saa.2019.04.008
Reference:	SAA 17016
To appear in:	*Spectrochimica Acta Part A: Molecular and Biomolecular Spectroscopy*
Received date:	26 December 2018
Revised date:	5 April 2019
Accepted date:	6 April 2019

Please cite this article as: H.T. Theint, J.E. Walsh, W.S. Tung, et al., Development of an optical biosensor for the detection of Trypanosoma evansi and Plasmodium berghei, Spectrochimica Acta Part A: Molecular and Biomolecular Spectroscopy, https://doi.org/10.1016/j.saa.2019.04.008

Development of an Optical Biosensor for the Detection of *Trypanosoma evansi* and *Plasmodium berghei*

Hay Thi Theint[1], James Edward Walsh[2], Wong Siew Tung[1], Kenny Voon Gah Leong[1] and Mahendran Shitan[3]

[1]Pathology Department, International Medical University, Kuala Lumpur Malaysia
[2]Centre for Pre-University Studies, International Medical University, Kuala Lumpur Malaysia
[3]School of Mathematical and Computer Sciences, Heriot-Watt University, Putrajaya, Malaysia

Corresponding author:
Dr James Edward Walsh,
Head of Centre for Pre-University Studies,
International Medical University (IMU)
No. 126, Jln Jalil Perkasa 19, Bukit Jalil, 57000 Kuala Lumpur, Malaysia
DID: +603-2731-7234 Mobile: +6017-687-4031 Fax: +603 8656 7229
E-mail: jameswalsh@imu.edu.my

Abstract

A laboratory prototype system that correlates murine blood absorbance with degree of infection for *Plasmodium berghei* and *Trypanosoma avensi* has been designed, constructed and tested. A population (n=6) of control uninfected, Plasmodium infected and Trypanosoma infected BALB/c mice were developed and spectral absorption measurements pre and post infection were made every 3 days. A fibre optic spectrometer set-up was used as the basis of a laboratory prototype biosensor that uses the Beer Lambert Law to relate Ultraviolet–Visible–Near-infrared absorbance data to changes in murine blood chemistry post infection. Spectral absorption results indicate a statistically relevant correlation at a 650 nm with infection for Plasmodium from between 4 and 7 sampling days' post infection, in spite of significant standard deviations among the sample populations for control and infected mice. No significant spectral absorption change for Trypanosoma infection was been detected from the current data. Corresponding stained slides of control and infected blood at each sampling date were taken with related infected cell counts determined and these correlate well for Plasmodium absorbance at 650 nm.

Keywords: Biosensor, Absorbance, Spectroscopy, Plasmodium, Trypanosoma

1. Introduction

Human population infected by blood pathogens such as *Plasmodium berghei* and *Trypanosoma avensi*, viruses such as dengue, hepatitis, HIV and a broad range of bacteria are currently a significant public health issue globally and in Malaysia [1-4]. Malaria, in particular, leads to an estimated half a million deaths annually worldwide [5]. It is a potentially life threatening disease caused by the widely distributed Plasmodium protozoan parasite [6]. In addition, Plasmodium is pathogenic to a variety of vertebral hosts, including primates, rodents, birds, and lizards. Surprisingly, humans are the only host who suffered from severe diseases caused by Plasmodium. Malaria remains one of the most significant burden diseases in Sub-Saharan Africa, affecting people with the complications of cerebral malaria [7]. Recent reports show that Malaysia has the highest incidence of *Plasmodium knowlesi* infection in the world [8]. Therefore, early detection of malaria has been the subject of intense scientific research investigation over the past decades due to its high transmission, morbidity and mortality rate.

On the other hand, Trypanosoma species are the major cause of Chagas disease and African trypanosomiasis or sleeping sickness. While epidemics of sleeping sickness have been a significant

public health problem in the past, ongoing trypanosomiasis has been a significant public health problem with 7,000-10,000 cases annually in recent years [9]. Similar to malaria, early detection allows safer medication to be applied and reduces death rates, so routine screening of the exposed potential population is required [10].

Conventional screening methods such as rapid diagnostic test (RDT) and the card agglutination test (CATT) are widely used as screening tests to diagnose malaria and trypanosomiasis across the world [11, 12]. Studies have shown that these tests have their own limitations [13, 14]. Many studies are trying to develop a reliable, rapid, inexpensive and portable device to overcome some of those limitations [15, 16], and to the best of our knowledge, detection of Plasmodium and Trypanosoma parasites by using Ultraviolet–Visible–Near-infrared (UV–Vis–NIR) absorbance optical biosensors remains relatively unstudied [15-33].

There have been several studies on the detection of a wide range of analytes including viruses, toxins, drugs, antibodies, tumour biomarkers and tumour cells using optical biosensors [15]. Optical biosensors allow easy-to-use, rapid, portable, multiplexed, and cost-effective diagnosis when compared to other sensors types [16] and it has been shown that changes in a biological component can be detected using light absorption [15]. Due to the lysing of red blood cells in malarial diseases, changes in blood cell parameters are well a known feature of this infection [17]. Therefore, it is logical that spectral absorbance measured with an optical biosensor can detect changes due to Plasmodium infected blood in its early stages. However, unlike Plasmodium, Trypanosoma does not lyse blood cells and may therefore produce different spectral absorbance changes.

Blood pathogen detection by spectroscopic methods is based on the principle that the infecting agent cause the blood products to break down with a resulting change in the biochemistry of the sample that alters its spectral absorbance [17]. Murine Trypanosomiasis and Plasmodium malaria infection will therefore be used as an example for this type of spectroscopic identification and quantification but the same general principles and techniques apply to a broad range of other blood pathogens [15, 16].

Optical sensing techniques can provide the required specifications for rapid, inexpensive and easy to use blood pathogen detection mechanisms based on related spectral changes cause by alterations in blood chemistry [15-18]. Spectral fingerprinting of biological and environmental analytics for detection and quantification is a well-established scientific technique and can be applied to infected blood samples provided that there are measurable spectral changes caused by the pathogen's effect on blood chemistry [34, 35]. The spectral changes that can occur in infected blood may be directly detectable by measuring the absorption spectra of control and infected blood samples or it can be based on applying a biochemical assay to the samples to produce a secondary spectral effect such as fluorescence. While the latter may provide better detection limits, the required assays before spectral detection can be complex and time consuming [19, 20]. Direct quantification of whole blood sample absorbance changes that are related to factors such as presence and degree of infection, time since initial infection and possibly even type and strain of infectious agent can provide a much simpler and less expensive approach as it involves no complex assaying [21, 22]. Ideally, there should be significant absorbance changes occurring post-infection in key spectral regions, such as the UV–Vis–NIR wavebands, that are related to specific target infection metrics and not to other potential co-factors such as age, medical history or presence of other infectious agents. The limit of detection for spectral monitoring of infected blood will be a function of factors, such as the spectral variation in baseline healthy blood and temporal changes in blood chemistry post extraction, that are unrelated to the infection in question. The determination of an accurate inter and intra subject baseline and the related time window for observation is therefore a key metric in this research.

There are a number of studies that examine aspects of parasite infection using UV–Vis–NIR spectroscopy [22, 23] but further work to determine the viability of these spectral wavebands for

frontline early detection of blood pathogens is required. Other techniques such chemiluminescence, Fourier Transform Infrared Spectroscopy (FTIR) and related Raman spectroscopy can also have significant pathogen specific spectral information and high limits of detection but the related pre-assaying and detection technologies can be quite complex and expensive [20, 21, 24]. More recently label free, rapid screening technique, Raman spectroscopy has been used for the characterisation/diagnosis of healthy and dengue infected human blood plasma samples [25]. There are extensive examples of the absorbance spectrum of various types of haemoglobin in the literature [36-41] and Firdous *et al* 2012 found that two prominent peaks in 500 – 6000 nm spectral region were observed for as a result of dengue infection of whole blood using relatively straight forward and inexpensive UV–Vis–NIR absorbance technology [22]. The development of a low cost spectral absorbance technique that can detect pathogens in freshly extracted whole blood is the basis for the research presented in this paper.

2. Materials and methods

2.1 Protocol for mouse infection data

6-8 weeks old female BALB/c mice were used in this experiment under IMU ethics approval 4.7/JCM-155/2018. Before the start of the experiment, cryopreserved *Plasmodium. berghei* and *Trypanosoma evansi* stored in liquid nitrogen were thawed and injected each into a BALB/c mouse intraperitoneally. Phosphate buffered saline (PBS) was used to obtain the desired number of parasites. In the order 1 x 10^6 *P. berghei* parasites were injected into each mouse in the Plasmodium group (n = 6) and a counted number of 50 *T. evansi* were introduced into each mouse from the Trypanosoma group (n = 6). For the control group (n = 6), 0.5 mL of PBS was introduced to simulate complications from injection. Once the presence of considerable amount of parasites was observed, the blood was collected by cardiac puncture method for experimental analysis and the infected mice were sacrificed by using diethyl ether. Once the infected blood was collected, calculations were made by using WHO counting method for *Plasmodium* and haemocytometer for *Trypanosoma.*

The testing of blood samples was performed in the morning of every 3rd day with day 1 being the day prior to infection and day 4 being 2 days' post-infection. On each sampling day blood was collected from tail incisions from each of the two infected and control populations (n = 6) and whole blood was placed in a specially designed sample holder, typically within 30 seconds to ensure a close *in-vivo* approximation. For each sample measurement a drop of blood, ~50 µL, was required to ensure the specially designed the sample holder was filled. In addition, photomicrographs of Giemsa stain blood were taken each sampling day from the 2 infected mouse populations and the control (x1000 magnification) to compare to the results of contemporaneous spectral absorbance date and provide quantitative information on infections levels. The parasitemia of Plasmodium infected mice was determined using the WHO malaria parasite calculation method. The parasitemia of Trypanosoma infected mice was determined by counting the total number of trypanosome parasites from n = 10 randomly chosen microscopic fields (x2000) and followed by calculation of the mean [42, 43].

2.2 Optical set up to determine absorbance of mouse blood.

An optical set-up was designed, constructed and tested in line with the system outlined in the Firdous *et al* 2012 [23] as shown in Figures 2.1. The optics components used are all Ocean Optics fibre optic spectroscopy components (Ocean Optics, USA). An optically stable HL-2000-HP broadband UV–Vis–NIR Tungsten lamp that was coupled via a 600 µm diameter fibre optic (QP-600-2-XSR) to a collimating lens (COL-UV-30) that was used to uniformly illuminate a 2 mm sample area from above the sample stage. An inverted 96 well plate cover was used as a short path length sample holder due it's shallow depth, given that blood is quite opaque in the visible and ultraviolet, with a cover slip

placed on top to ensure uniform blood sample depth and volume. As the depth of the cells on the 96 well plate cover was 0.4 mm (+/- 0.1) and the diameter 8.5 mm (+/- 0.5) the resulting volume is approximately 22.5 µl. The well plate sample holders were then placed central to the 2 mm diameter sampling light beam on a horizontally mounted cuvette holder (CUV-UV). Another 600 µm diameter fibre optic (QP-600-2-XSR) and collimating lens (COL-UV-30) couple the light from the sample area to an Ocean Optics Maya 2000 spectrometer where the resulting UV–Vis–NIR spectra are acquired (Ocean Optics, USA).

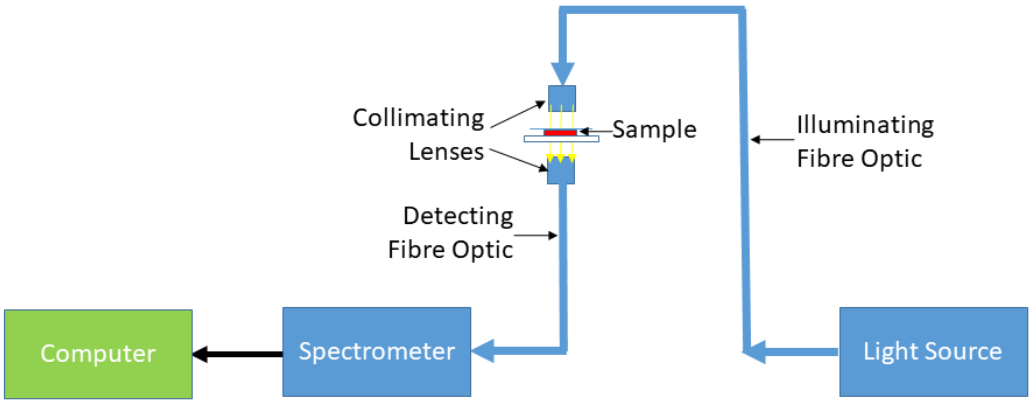

Figure 2.1. Schematic diagram of the key components of the optical system for measuring the UV–Vis–NIR spectral absorbance of control, Plasmodium and Trypanosoma infected mouse blood after Firdous *et al* 2012 [23].

`

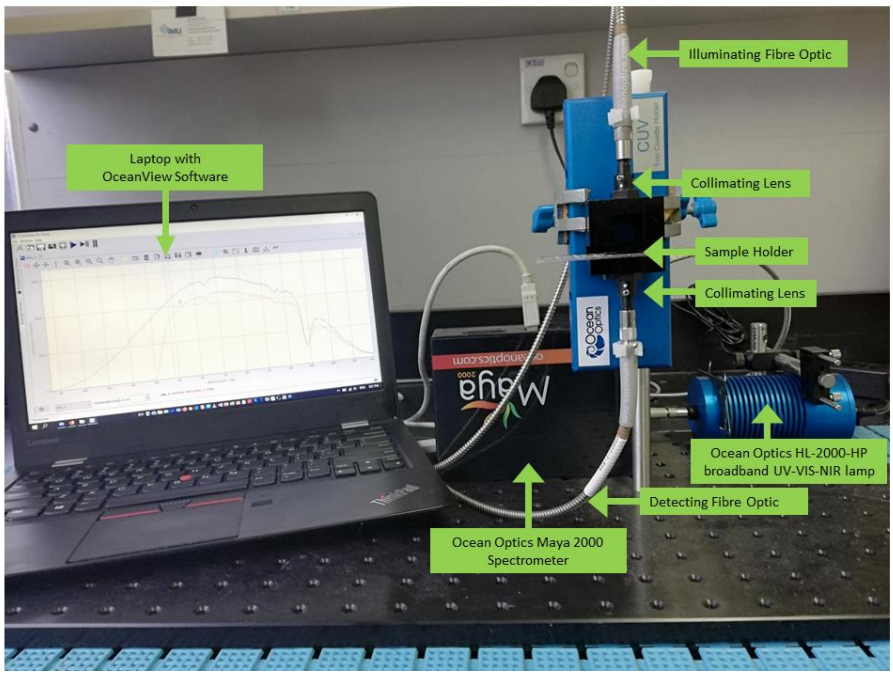

Figure 2.2. Experimental setup of the key components of the optical system for measuring the UV–Vis–NIR spectral absorbance of control, Plasmodium and Trypanosoma infected mouse blood.

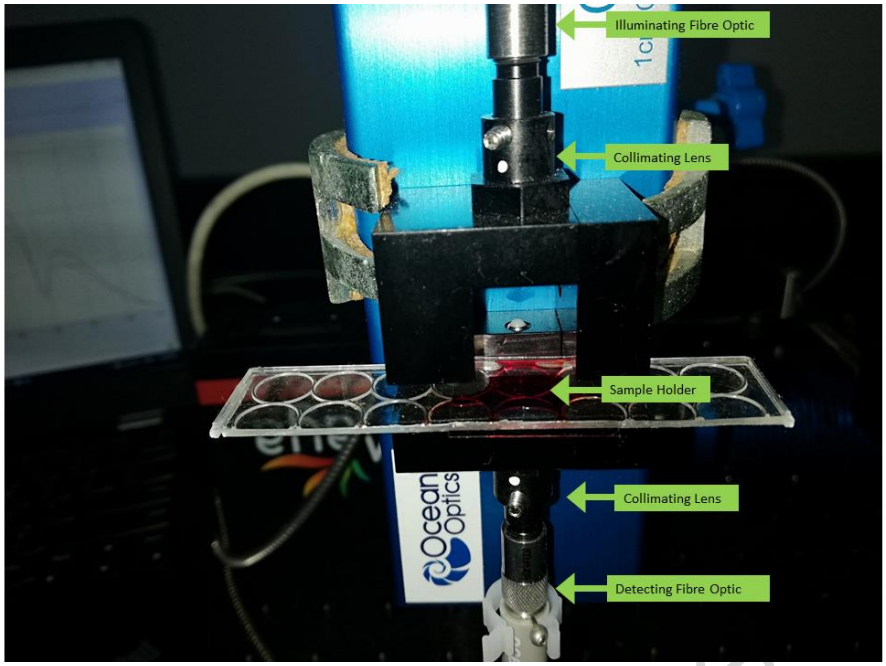

Figure 2.3. Sample holder set-up, comprising an inverted 96 well plate cover and cover slip, for measuring the UV–Vis–NIR spectral absorbance of control, Plasmodium and Trypanosoma infected mouse blood samples, with a 0.4 mm (+/- 0.1) optical path length and approximately 22.5 µl volume.

The settings of spectrometer acquisition software were 15 ms integration time per scan, with 100 scans per spectrum and with dark subtraction applied to maximize signal to noise. Spectral intensity data in the UV–Vis–NIR wavebands is then read into a computer running the OceanView spectrometer software and transmittance, T(λ), or absorbance, A(λ), is computed for later analysis. Transmittance and Absorbance spectra of the sample are computed by comparing the spectrum of the lamp at each wavelength, λ, when no blood sample is present, $I_o(\lambda)$, to the signal emanating from a blood sample, I(λ). The Beer-Lambert law then allows the resulting absorbance or transmittance spectra to be related to specific sample parameters such as a concentration, c, and molar absorption coefficient, ε(λ), for a fixed path length, l, according to equation 2.1. For the measurement setup shown in Figures 2.2 and 2.3, the optical path length, l, is determined by the 0.4 mm (+/- 0.1) depth of the inverted 96 well plate cover capped by the cover slip. Therefore, absorbance changes should occur if blood chemistry (i.e. ε(λ)) and/or concentration vary. Any concentration variation should not have a spectrally varying component across the UV–Vis–NIR but will just affect the overall absorbance at each wavelength.

$$A(\lambda)= \log (1 /T(\lambda)) = \log (I_o(\lambda) /I(\lambda)) = \varepsilon(\lambda)cl$$

Equation 2.1

The optical set-up was calibrated using known coloured absorption filters with stated spectral transmittance in UV–Vis–NIR. A Roscolux, R27, Medium Red filter (Roscolux, USA) was considered to be the closest approximation of blood colour and was therefore used to test the system Blood absorbance [36-41]. Once calibration using the Roscolux Medium Red filter was confirmed as shown in figure 2.4, control and infected blood samples from the mice were tested.

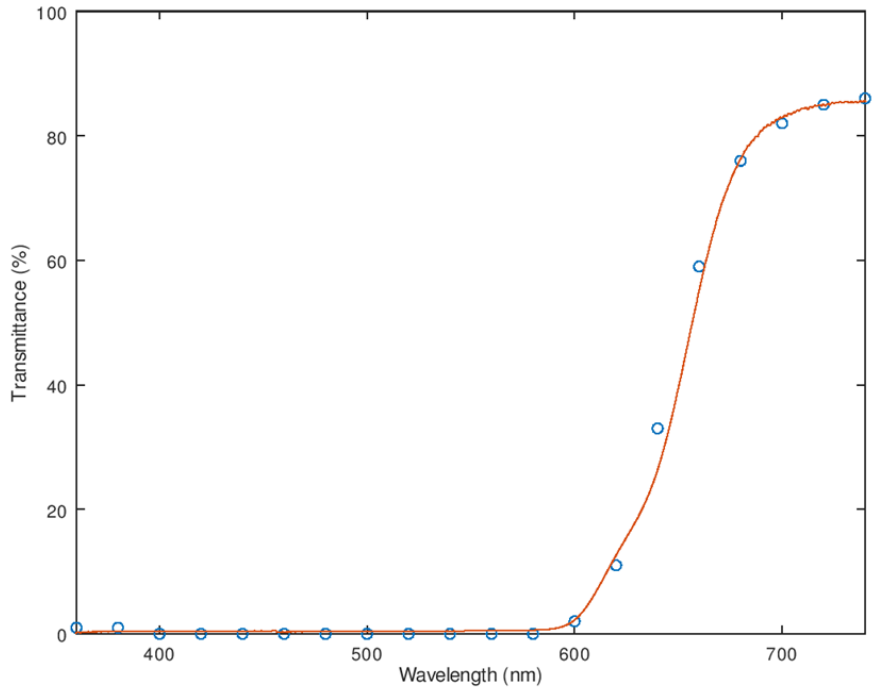

Figure 2.4. Transmission spectrum of a Roscolux, R27, Medium Red filter (Roscolux, USA) as measured by the optical setup shown in Figure 2.3 (—), manufacturer's data given every 20 nm is overlaid (o).

For the mouse blood spectra, 5 samples were measured for each of the n = 6 mice from the Plasmodium, Trypanosoma and control populations, this allows us to quantify the intra-mouse variation as well as the inter-mouse variation across the population (n = 6). In addition, the lamp output spectrum, $I_o(\lambda)$, was monitored on each sampling day to ensure the stability of the optical setup over the lifetime of the experiment.

3. Results

3.1 Microscopic slide examination

Figures 3.1 to 3.5 show photomicrographs (x2000) of each population of mice, Plasmodium and Trypanosoma infected and the control taken on each of the 5 sampling dates. Figure 3.1 shows microscopic blood examination of control, Plasmodium and Trypanosoma mice blood on day 1 with all presenting healthy red blood cells as per the control and no sign of pathogen can be seen in slides (b) and (c) as expected. The intended mouse populations for Plasmodium and Trypanosoma infection were inoculated the following day (i.e. day 2). On day 4, which is 2 days after infection, and day 7 the respective microscope pictures in Figures 3.2 and 3.3 show no sign of trophozoites and trypomastigotes in slides (b) and (c). In Figure 3.4 trophozoites and trypomastigotes can start be seen in in slides (b) and (c) on day 10, with significant evidence of infection visible on day 13 in Figure 3.5 slides (b) and (c). The photomicrographs in Figures 3.1 to 3.5 are qualitative to indicate the presence of infection, cell counting methods provide the quantitative data for correlation with the spectral data [42, 43].

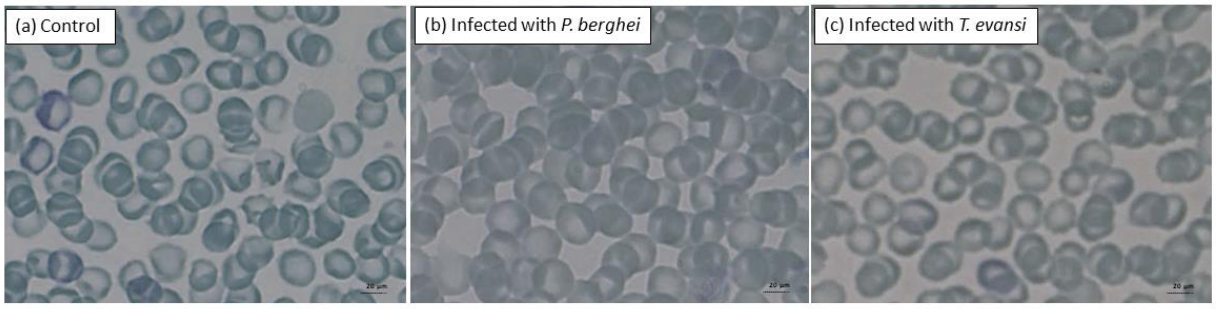

Figure 3.1. Photomicrographs of Giemsa stain blood film on day 1 pre infection: (a) Control (b) Uninfected with *P. berghei* (c) Uninfected with *T. evansi* (x2000 magnification)

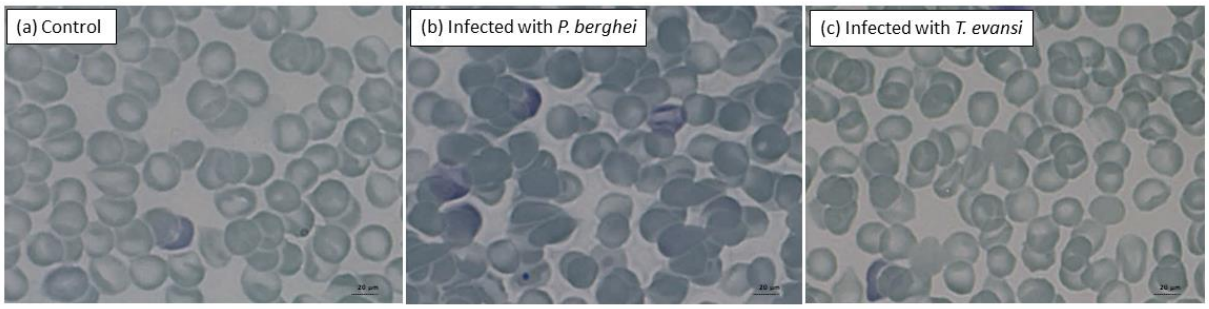

Figure 3.2. Photomicrographs of Giemsa stain blood film on day 4 post infection: (a) Control (b) Infected with *P. berghei* (c) Infected with *T. evansi* (x2000 magnification)

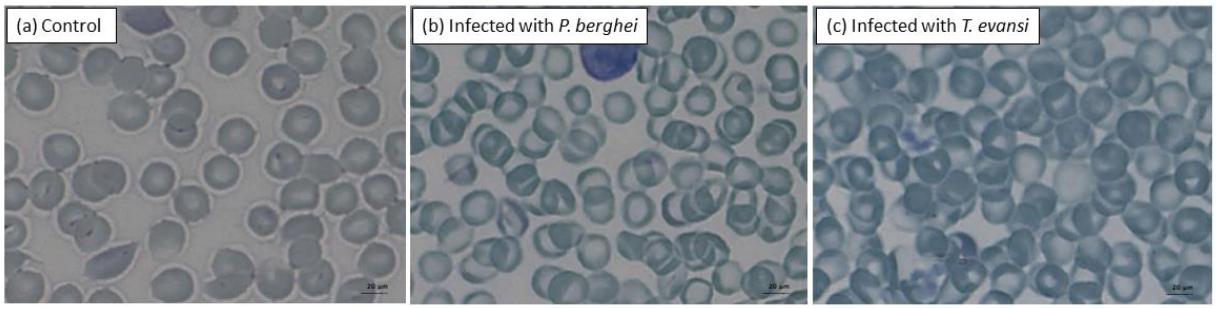

Figure 3.3. Photomicrographs of Giemsa stain blood film on day 7 post infection: (a) Control (b) Infected with *P. berghei* (c) Infected with *T. evansi* (x2000 magnification)

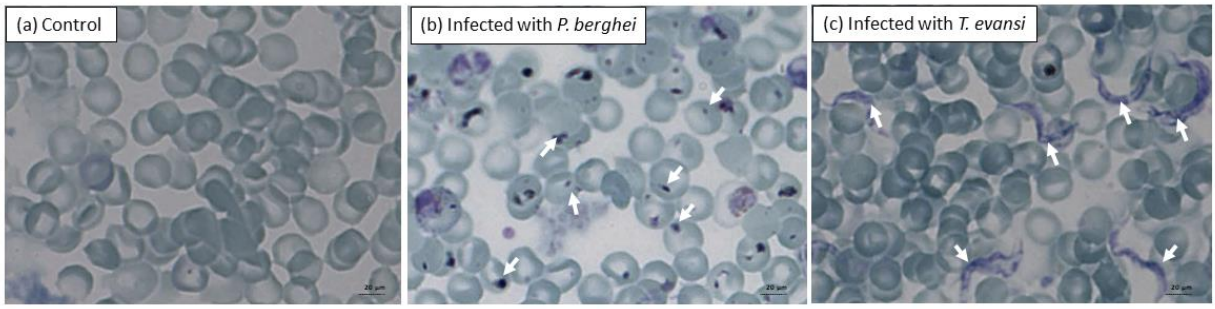

Figure 3.4. Photomicrographs of Giemsa stain blood film on day 10 post infection: (a) Control (b) Infected with *P. berghei* (c) Infected with *T. evansi* (x2000 magnification)

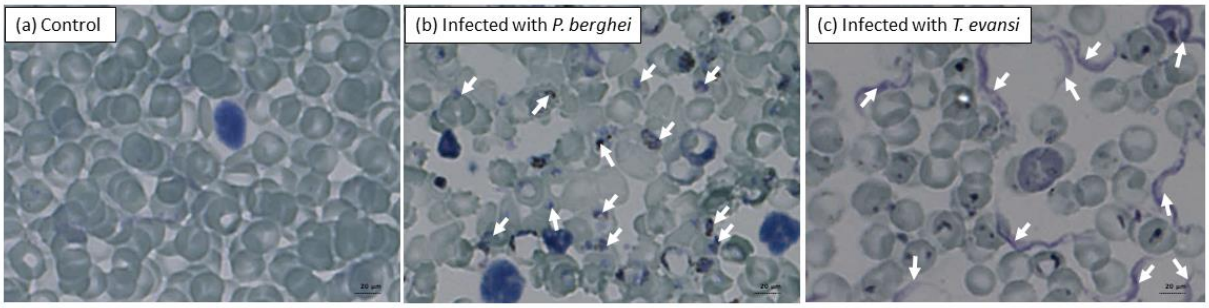

Figure 3.5. Photomicrographs of Giemsa stain blood film on day 13 post infection: (a) Control (b) Infected with *P. berghei* (c) Infected with *T. evansi* (x2000 magnification)

Tables 3.1 and 3.2 show the increase in parasite count post infection for Plasmodium and Trypanosoma respectively which indicates varying degrees of infection by day 13. The WHO method was applied for Plasmodium [42] and for Trypanosoma the number parasites were averaged across 10 randomly sampled fields (x2000) [43]. The presence of the infectious agents only presented in the blood cell micrographs from day 10, probably due to the life cycle and aetiology of Plasmodium and Trypanosoma. There is a standard deviation of around 16% across the 10 randomly sampled fields for each Trypanosoma infected mouse but the variance across the related infected mouse population (n = 6) is very large. The standard deviation for the WHO method applied to the Plasmodium infected mouse group is considerably smaller. Trypanosoma and Plasmodium are two totally different blood parasites in which Trypanosoma evansi are found extracellularly (outside of the blood cells) whereas Plasmodium berghei are intracellular parasites found inside the RBC. Thus, the mechanism of pathophysiology of these two parasitic infection would be different. The amount or load of parasites used in this study was based on the literature review where other researchers have optimised the number of parasites for infecting the animals.

	Plasmodium infected mouse	Day 1	Day 4	Day 7	Day 10	Day 13
Plasmodium (parasitaemia per µL)	1	0	0	0	312,452	778,475
	2	0	0	0	347,235	724,643
	3	0	0	0	301,242	705,368
	4	0	0	0	345,264	743,634
	5	0	0	0	325,573	744,864
	6	0	0	0	322,232	763,796
	Average	0	0	0	325,666	743,463
	Std.Dev.	0	0	0	18,068	26,255

Table 3.1. Parasitaemia of Plasmodium infected mice determined by microscopic method from the WHO [42].

	Trypanosoma infected mouse	Day 1	Day 4	Day 7	Day 10	Day 13
Trypanosoma (parasitaemia per field)	1	0	0	0	30	68
	2	0	0	0	15	52
	3	0	0	0	14	32
	4	0	0	0	0	12
	5	0	0	0	5	10
	6	0	0	0	1	9
	Average	0	0	0	11	31
	Std.Dev.	0	0	0	12	26

Table 3.2. Parasitaemia of Trypanosoma infected mice determined by microscopic method with a x2000 field [43].

3.2 Spectral absorbance measurement

For each mouse in the population (n = 6) across the two infected and control populations five spectra from distinct blood samples were measured each day in addition to the light source to ensure the optical set-up was stable. Typical spectral intensity data for the lamp on each of the five sampling days and a control mouse on day 1 are shown in Figure 3.6. For this data typical lamp spectra on each of the five sampling days are overlaid to show that the optical set-up remained sufficiently stable (+/-1%) over the lifetime of the 13-day experiment. While the overlaid control blood spectra recorded on day 1 for the same mouse indicate the typical inter-mouse spectral variance (+/-1%) for five concurrent samples (n = 5). The lamp intensity spectra ($I_0(\lambda)$ and blood intensity spectra ($I(\lambda)$ and are used to calculate spectral absorbance and can therefore be related to blood chemistry, using the Beer Lambert in equation 2.1.

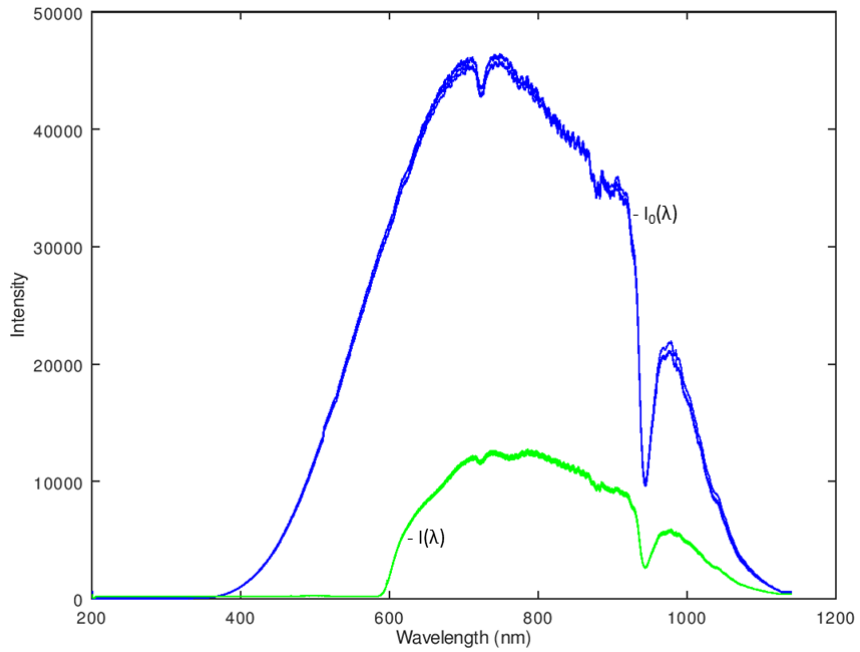

Figure 3.6. Typical spectral intensity for the lamp on each of the five sampling days (blue) and for concurrent samples (n = 5) of a control mouse blood on day 1 (green).

Figure 3.7 shows the average absorbance spectral for the control mice (n = 6) on each of the five sampling dates which indicates the baseline absorbance spectrum was reasonably constant. Figure 3.8 shows the average of the concurrent absorbance spectra for the Plasmodium infected mice (n = 6) on each of the five sampling dates which indicates that the absorbance spectra were initially similar to that of the control baseline but an increase in absorbance in the 650 nm region occurred as the infection progressed. Figure 3.9 shows the average absorbance spectral for the Trypanosoma infected mice (n = 6) on each of the five sampling dates which indicates that the absorbance spectra were largely similar to that of the control baseline in the 650 nm spectral region and with no other significant spectral change evident in the data as presented. The absorbance date below 600 nm is quite variable for all samples but no significant correlation was found with time since infection in this spectral region apart from day 13 for Plasmodium when significant increases in absorbance occurred at 440 nm, 550 nm and 575 nm. Given the low light intensity levels below 600 nm for the highly absorbing blood and the lower lamp output in this spectral region, as shown in Figure 3.6, a very low signal to noise ratio can be expected below 600 nm, causing apparent saturation of the absorbance data, thus making the data in this spectral region quantitatively unreliable for the current optical set-up.

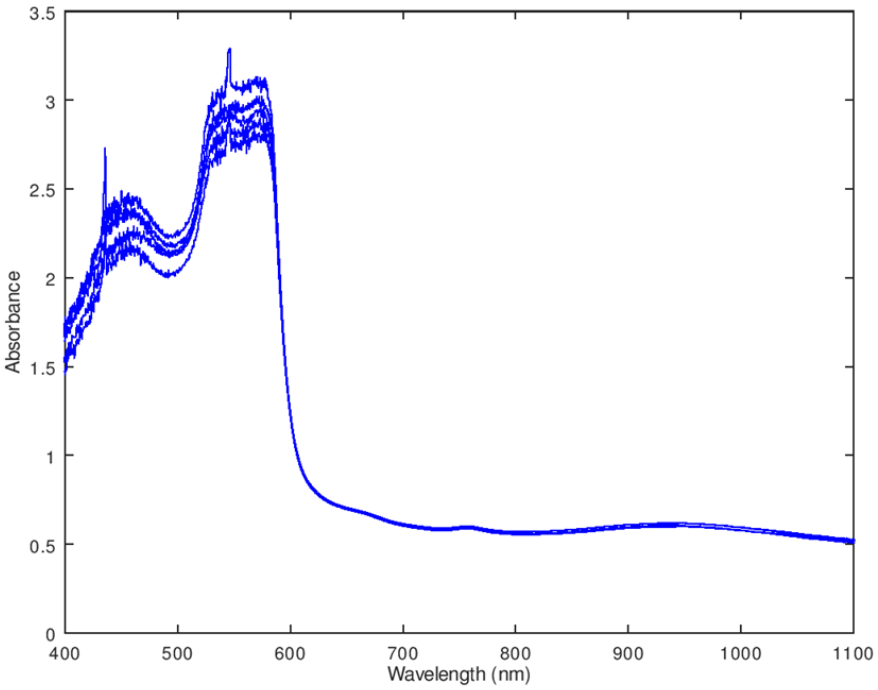

Figure 3.7. The average absorbance spectral for the control mice (n = 6) on each of the five sampling dates.

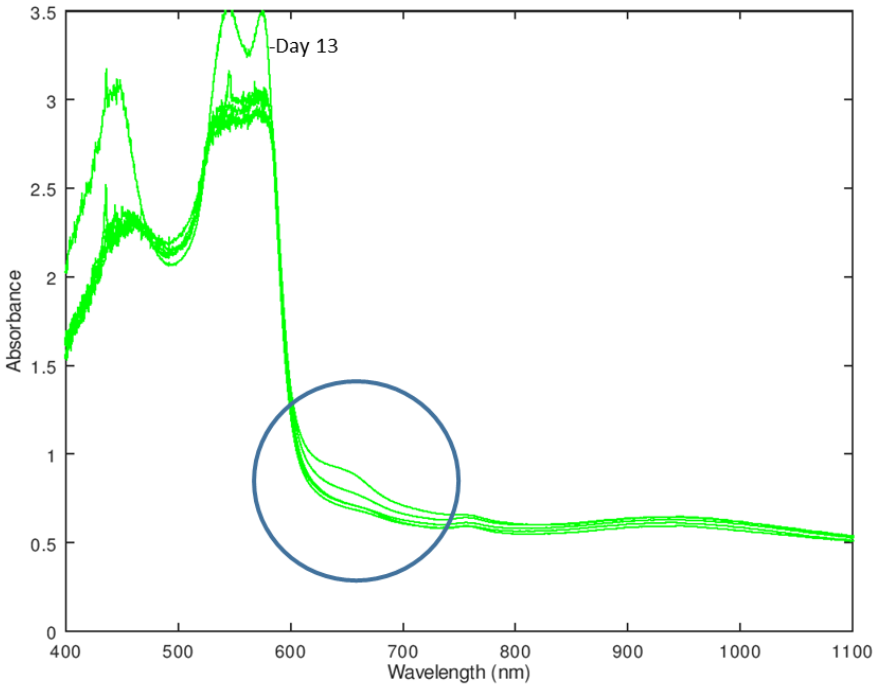

Figure 3.8. The average absorbance spectral for the Plasmodium infected mice (n = 6) on each of the five sampling dates showing significant absorbance variation at 650 nm and in peaks below 600 nm on day 13.

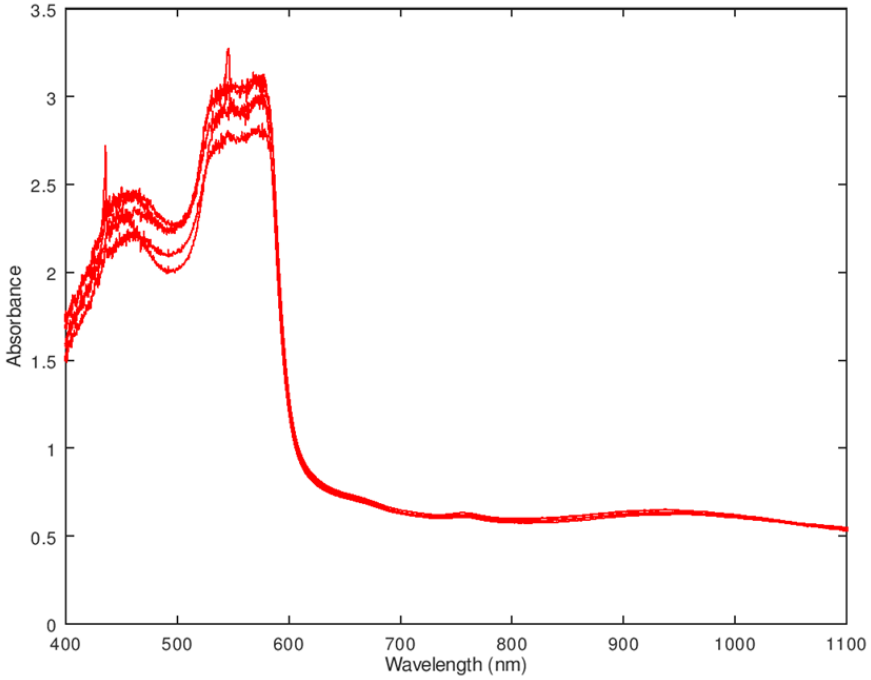

Figure 3.9. shows the average absorbance spectral for the Trypanosoma infected mice (n = 6) on each of the five sampling dates.

Based on the spectral data in Figures 3.7 to 3.9 a statistical analysis was carried out on the absorbance at 650 nm for all three mouse populations. Figure 3.10 shows the absorbance of the control population over the 5 sampling dates at 650 nm which determines the baseline in this spectral region. Figure 3.11 shows the absorbance of the Plasmodium infected population over the 5 sampling dates at 650 nm which indicates a significant increase in absorbance as the infection progresses, particularly on days 10 and 13, as indicted in table 3.1. Figure 3.12 shows the absorbance of the Trypanosoma infected population over the 5 sampling dates at 650 nm which indicates no similar significant increase in absorbance as the infection progresses, as indicted in table 3.2. Similar analysis was carried out on the absorbance features that are evident below 600 nm for all 3 mouse populations but no significant trend was found over the 5 sampling dates apart from plasmodium on day 13.

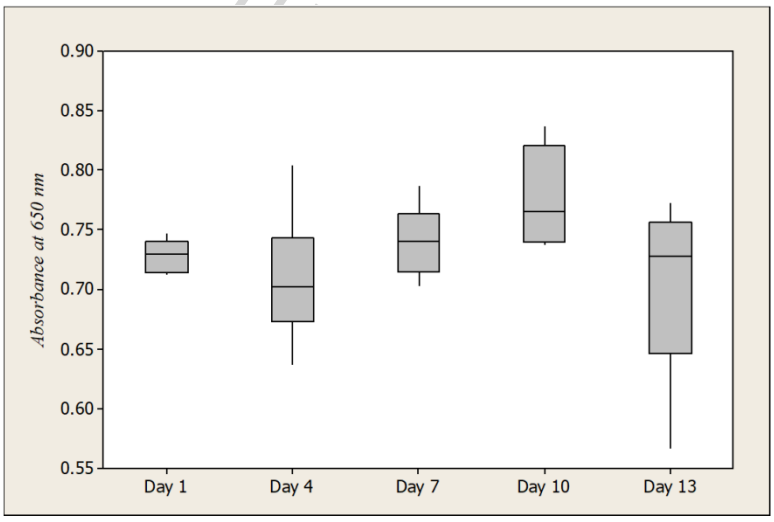

Figure 3.10. Boxplot of absorbance at 650 nm for the sample mice (n = 6) for the control group.

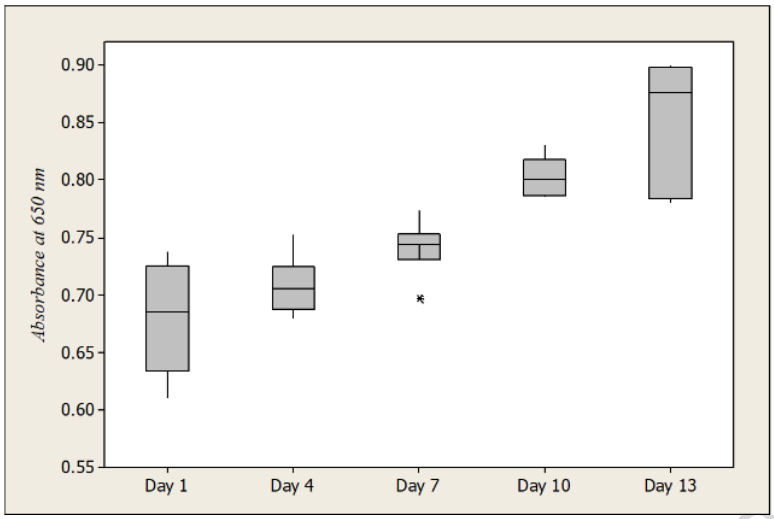

Figure 3.11. Boxplot of absorbance at 650 nm for the sample mice (n = 6) for the Plasmodium group.

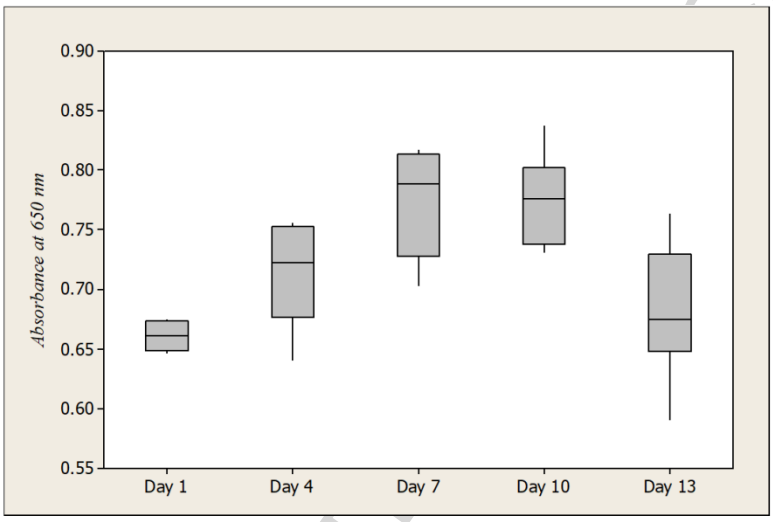

Figure 3.12. Boxplot of absorbance at 650 nm for the sample mice (n = 6) for the Trypanosoma group.

The data in Figure 3.11 for plasmodium absorbance at 650 nm compares favourably with the infection level data presented in Table 3.1 and is correlated in Figure 3.13. However, as the cell counting methods used for the infectious agents failed to quantify any infection levels on days 4 and 7, the correlation is carried using the data from Days 1, 10 and 13 and linear calibration curve applied. For Trypanosoma the variance across the infected mouse population on days 10 and 13 was too great to provide a reliable absorbance calibration.

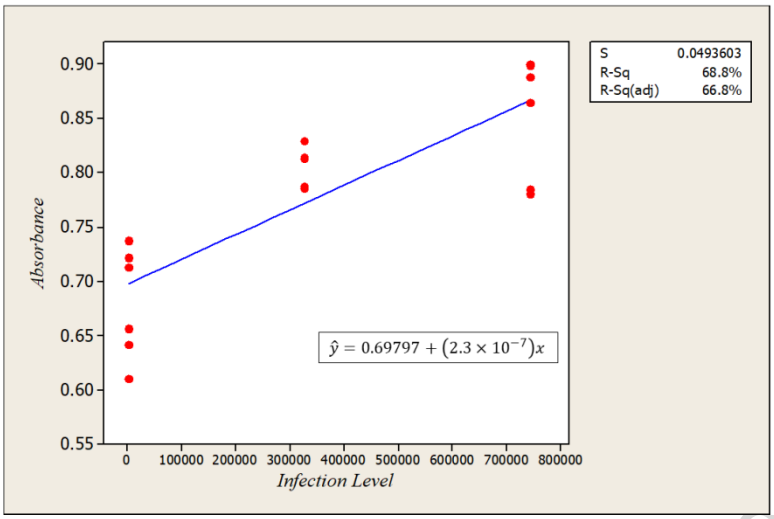

Figure 3.13. Plasmodium infected blood absorbance at 650 nm versus infection level on sampling days 1, 10 and 13.

4. Discussion

From the graph of Boxplot for the Plasmodium group in Figure 3.11, we can clearly see that there is an upward shift in the distribution of the data over time. Hence, we naturally we would like to determine if there is a significant difference in the central location (median) of the data with respect to time. The data does not appear to be normally distributed with equal variances and the sample size in this study, $n = 6$ is rather small. Since the assumptions for traditional statistical analysis are not met, we preferred to apply the non-parametric test namely, Sign Test to determine whether or not there has been a significant difference in the median over time.

In order to conduct the test, let α_k denote the median for Day_k (k = 1, 4, 7, 10, 13) and the hypothesis is formulated as follows:

H_O: $\eta_k - \eta_1 = 0$, [There is no difference in the median between Day_k and Day_1]

H_A: $\eta_k - \eta_1 > 0$, [Median of Day_k is greater than Day_1] (k = 4, 7, 10, 13)

Table 4.1. Sign test results for Plasmodium absorbance data at 650 nm.

Variable	*n*	Below 0	Above 0	*p*-value	Median	Lower Confidence Level	Upper Confidence Level
$\text{Day}_4 - \text{Day}_1$	6	3	3	0.6563	0.0235	− 0.0230	0.0867
$\text{Day}_7 - \text{Day}_1$	6	1	5	0.1094	0.0690	− 0.0143	0.1266
$\text{Day}_{10} - \text{Day}_1$	6	0	6	0.0156	0.1260	0.0586	0.1859
$\text{Day}_{13} - \text{Day}_1$	6	0	6	0.0156	0.1570	0.0836	0.2734

The α-level was set 0.05 and the results of the tests are listed in Table 4.1.

The *p*-values are listed out in column 5 of Table 4.1 and we notice that the *p*-value for the difference of the median between Day_4 and Day_1 is 0.6563 which is greater than 0.05, thus rendering insufficient evidence to reject H_O. Similarly, the *p*-value for the difference of the median between Day_7 and Day_1 is 0.1094 which is also greater than 0.05, thus again rendering insufficient evidence to reject H_O.

However, for the other days (i.e. difference of the median between Day_k (k = 10, 13) and Day_1, the *p*-values are smaller than 0.05 indicating there is sufficient evidence to reject H_O. We therefore, conclude that there are significant differences of the median between Day_k (k = 10, 13) and Day_1.

In addition, in columns 7 and 8 of Table 4.1, the 95% Sign Confidence Intervals for the median are listed out. Observe that the value of zero is not contained in the 95% confidence intervals for differences of the median between Day_k (k = 10, 13) and Day_1 thus indicating that there are significant differences and an upward shift has occurred.

A similar statistical analysis was also undertaken for the Trypanosoma group. From the graph of Boxplot in Figure 3.12, we can clearly see that there is an upward shift in the distribution of the data until Day_{10} and then a drop for Day_{13}.

Thus the hypothesis are formulated as follows for k = 4, 7, 10 only.

H_O: $\eta_k - \eta_1 = 0$, [There is no difference in the median between Day_k and Day_1]

H_A: $\eta_k - \eta_1 > 0$, [Median of Day_k is greater than Day_1] (k = 4, 7, 10)

The α-level was set 0.05 and the results of the tests are listed out in Table 4.2. The *p*-values are listed out in column 5 of Table 4.2 and we notice that the *p*-value for the difference of the median between Day_4 and Day_1 is 0.1094 which is greater than 0.05, thus rendering insufficient evidence to reject H_O.

Table 4.2. Sign test results for Trypanosoma absorbance data at 650 nm.

Variable	*n*	Below 0	Above 0	*p*-value	Median	Lower Confidence Level	Upper Confidence Level
$Day_4 - Day_1$	6	1	5	0.1094	0.0605	− 0.0018	0.0983
$Day_7 - Day_1$	6	0	6	0.0156	0.1230	0.0620	0.1510
$Day_{10} - Day_1$	6	0	6	0.0156	0.1095	0.0834	0.1543

However, for the other days (i.e. difference of the median between Day_k (k = 7, 10) and Day_1, the *p*-values are smaller than 0.05 indicating there is sufficient evidence to reject H_O. We therefore, conclude that there are significant differences of the median between Day_k (k = 7, 10) and Day_1.

In addition, in columns 7 and 8 of Table 4.2, the 95% Sign Confidence Intervals for the median are listed out. Observe that the value of zero is not contained in the 95% confidence intervals for differences of the median between Day_k (k = 7, 10) and Day_1 thus indicating that there are significant differences and an upward shift has occurred until Day_{10}.

For the Plasmodium infected absorbance at 650 nm calibration curve in Figure 3.13, let y_i denote the absorbance reading and x_i the infection level (i = 1, 2, ...,13). A linear model, $y_i = \beta_0 + \beta_1 x_i + \varepsilon_i$, was fitted to the data set and the fitted line is given by $\hat{y} = 0.69797 + (2.3 \times 10^{-7})x$. Both the coefficients were found to be significant at the α = 0.05 level. The R^2 value and adjusted R^2 were found to be 68.8% and 66.8%, respectively.

5. Conclusions

A novel prototype laboratory set-up for measuring the absorbance of control, Plasmodium and Trypanosoma infected mouse blood has been designed, constructed and tested. The increasing level of absorbance at 650 nm suggests that the molar absorptivity of Plasmodium infected mice blood is changing due to the pathogenesis of the disease which affects red blood cells [28, 29]. The Plasmodium infected blood shows significant absorbance differences at 650 nm, from the control baseline blood, occur between day on 10, which is days' post infection. However, there is some evidence from Figure 3.11 and the corresponding p values (0.109) that the effect may be detectable sometime after day 7, which is 5 days' post infection.

Similarly, the microscopic cell counting methods applied showed no sign of Plasmodium infection until day 10. On the other hand, the absorbance at 650 nm for Trypanosoma infected blood shows no significant variation from the control baseline blood absorbance spectrum over the same sampling time period (i.e. 13 days). The disparity between these two results can be explained by the differing pathogenesis of respective infecting agents. Unlike Plasmodium which causes destruction of red blood cells, Trypanosoma targets the host's tissues and organs showing a multiplication of trypomastigotes [44]. The absorbance results for Plasmodium infected blood at 650 nm are also in line with stained microscope samples of the blood and the corresponding infection level assay data. For Trypanosoma the standard deviation in increasing infection levels by day 13 was very large for the given population (n = 6) using the method applied, an improved method needs to be applied in future. The changes in Plasmodium infected blood absorbance at 650 nm are correlated to the WHO infection level data, which provides an initial calibration curve for the optical system.

Based on the results to date, the next phase of the research will be to further analyse the existing absorbance data for normal and infected mice to see if any, as yet undetected, spectral signatures exist for Trypanosoma infection and further analyse Plasmodium infected absorbance to data. Particularly below 600 nm where the signal to noise for the optical system presented here was too low to determine any significant spectral signatures that correlate with either infection. Principles components methods such as Singular Value Decomposition can be applied in this regard to investigate all relevant regions of the absorbance spectra [45, 46]. From an experimental design perspective, the signal to noise of the system can be enhanced by increasing the light source intensity and using a more sensitive detection system that specifically targets the key features of the spectral signatures detected. For example, rather than use a generic spectrometer system such as the Ocean Optics Maya 2000, a wavelength specific illumination/detection optical system can be developed using high intensity LEDs and sensitive photodetectors. This next generation laboratory based optical

prototype can then form the basis for a commercial prototype system which can determine spectral signatures of blood, possibly in-vivo using fibre optic micro-probes [34, 35]. The key result from a second generation laboratory prototype would be to confirm the accuracy of the absorbance versus infection calibration curve shown in Figure 3.13 to improve the limit of detection and minimise the detection time post infection.

Acknowledgements

Funding for this research provided by IMU Research Project BMS I-2018 (06)

References

[1] Lim, V.K.E, 2009. Occupational infection *Malaysian J Pathol.* **31(1)** 1-9.
[2] Deris, Z.Z., Harun, A., Omar, M. and Johari, M.R., 2009. The prevalence and risk factors of nosocomial cinetobacter blood stream infections in tertiary teaching hospital in north-eastern Malaysia, *Tropical Biomedicine.* **26(2)** 123-129.
[3] Hamid, M.Z.A., Aziz, N.A., Anita, A.R. and Norlijah, O., 2010. Knowledge of blood-borne infectious diseases and the practice of universal precautions amongst health-care workers in a tertiary hospital in Malaysia, *Southeast Asian J Trop Med Public Health.* **41(5)** 1192-1199.
[4] Hesham. R., Tajunisah, M.E. and Ilina, I., 2008. Risk of blood-borne infection among health care workers in two Kuala Lumpur hospitals, *Med J Malaysia.* **63(3)** 222-223.
[5] Centers for Disease Control and Prevention, April 25th 2018. *World Malaria Day.* Retrieved from https://www.cdc.gov/features/worldmalariaday
[6] Collins, W. and Jeffery, G., 2007. *Plasmodium malariae*: Parasite and disease, *Clinical Microbiology Reviews.* **20(4)** 579-592
[7] Shikani, H., Freeman, B., Lisanti, M., Weiss, L., Tanowitz, H. and Desruisseaux, M., 2012. Cerebral malaria, *The American Journal of Pathology.* **181(5)** 1484-1492.
[8] Lum, M. June 25th 2017. Malaysia has the highest cases of monkey malaria, *The Star*. Retrieved from: https://www.star2.com/health/wellness/2017/06/25/dealing-monkey-malaria
[9] Centers for Disease Control and Prevention, August 29th 2012. *African Trypanosomiasis - Epidemiology & risk factors.* Retrieved from: https://www.cdc.gov/parasites/sleepingsickness/epi.html
[10] Bonnet, J., Boudot, C. and Courtioux, B., 2015. Overview of the Diagnostic methods used in the field for fuman African Trypanosomiasis: What could change in the next years?, *BioMed Research International*. **2015** 1-10.
[11] Centers for Disease Control, 2018. *Malaria Diagnosis (U.S.) – Rapid Diagnostic Test.* Retrieved from: https://www.cdc.gov/malaria/diagnosis_treatment/rdt.html
[12] Centers for Disease Control, 2018. *Resources for Health Professionals - Definitive Diagnosis Rests On The Observation Of Trypanosomes By Microscopy.* Retrieved from: https://www.cdc.gov/parasites/sleepingsickness/health_professionals/index.html
[13] Lejon, V., Ngoyi, D., Boelaert, M. and Büscher, P., 2010. A CATT negative result after treatment for human African Trypanosomiasis is no indication for cure, *PLoS Neglected Tropical Diseases.* **4(1)** e590.
[14] RDT Info., 2008. *Current information on rapid diagnostic tests.* Retrieved from: http://www.rapid-diagnostics.org/app_advan.htm
[15] Damborsky, P., Vitel, J. and Katrlik, J., 2016. Optical biosensors, *Essays In Biochemistry.* **60(1)** 91-100.
[16] Yoo, S. and Lee, S., 2016. Optical biosensors for the detection of pathogenic microorganisms, *Trends in Biotechnology.* **34(1)** 7-25.
[17] Capuano, R., Domakoski, A.C., Grasso, F., Picci, L., Catini, A., Paolesse, R., Sirugo, G., Martinelli, E., Ponzi, M. and Di Natale, C., 2017. Sensor array detection of malaria volatile signature in a murine model, *Sensors & Actuators: B.* **245** 341-351.
[18] Kotepui, M., Piwkham, D., PhunPhuech, B., Phiwklam, N., Chupeerach, C. and Duangmano, S., 2015. Effects of malaria parasite density on blood cell parameters, *PLoS ONE* **10(3)** e0121057.
[19] Chan, K., Tan, C., Teng, W., Rahman, F., Soon, S. and Zulkifly, Z., 2010. Feasibility study of song period grating as an optical biosensor for dengue virus detection – an alternative approach to dengue virus screening, *IEEE, EMBS Conference on Biomedical Engineering and Sciences (IECBES),* November 2010, Kuala Lumpur: IEEE.
[20] Atias, V., Liebesc, Y., Chalifa-Caspid, V., Bremande, L., Lobel, L., Mars, R. and Dussarte. P., 2009. Chemiluminescent optical fiber immunosensor for the detection of IgM antibody to dengue virus in humans, *Sensors and Actuators B.* **140(1)** 206-215.
[21] Rehman, A., Anwar, S., Firdous, S., Ahmed, M., Rasheed, R. and Nawaz, M., 2012. Dengue blood analysis by Raman spectroscopy, *Laser Phys.* **22(6)** 1085-1089.
[22] Firdous, S., Ahmed, M., Rehman, A., Nawaz, M., Anwar, S. and Murtaza, S., 2012. Transmission spectroscopy of dengue viral infection, *Laser Phys. Lett.* **9(4)** 317–321
[23] Serebrennikova, Y.M., Pate, J., Milhous, W.K., Garcia-Rubio, L.H., Huffman, D.E. and Smith, J.M., 2013. Spectrophotometric detection of susceptibility to anti- malarial drugs, *Malaria Journal.* **12** 305.

[24] Gobrecht, A., Bendoula, R., Roger, J. and Bellon-Maurel, V., 2015. Combining linear polarization spectroscopy and the Representative Layer Theory to measure the Beer–Lambert law absorbance of highly scattering materials, *Analytica Chimica Acta*. **853** 486-494.

[25] Mahmood, T., Nawaz, H., Ditta, A., Majeed, M. I., Hanif, M.A., Rashid, N., Bhatti, H.N., Nargis, H.F., Saleem, M., Bonnier, F. and Byrne, H.J., 2018 Raman spectral analysis for rapid screening of Dengue infection, *Spectrochim Acta A Mol Biomol Spectrosc.* **200** 136-142.

[26] Kaminski, T. and Geschwindner, S., 2017. Perspectives on optical biosensor utility in small-molecule screening, *Expert Opinion on Drug Discovery*, **12(11)** 1083-1086.

[27] World Health Organization, 2018. *Malaria Rapid Diagnostic Tests.* Retrieved from: http://www.who.int/malaria/areas/diagnosis/rapid-diagnostic-tests/en/

[28] Moore, L., Fujioka, H., Williams, P., Chalmers, J., Grimberg, B., Zimmerman, P. and Zborowski, M., 2006. Hemoglobin degradation in malaria-infected erythrocytes determined from live cell magnetophoresis, *The FASEB Journal.* **20(6)** 747-749.

[29] Masilamani, V., Devanesan, S., Ravikumar, M., Perinbam, K., AlSalhi, M., Prasad, S., Palled, S., Ganesh, K.M. and Alsaeed, A.H., 2014. Fluorescence spectral diagnosis of malaria – a preliminary study, *Diagnostic Pathology*. **9(1)** 182.

[30] Ragavan, K., Kumar, S., Swaraj, S. and Neethirajan, S., 2018. Advances in biosensors and optical assays for diagnosis and detection of malaria, *Biosensors and Bioelectronics*. **105** 188-210.

[31] Technische Universitat Darmstadt, 2012. Bioscientists develop a biosensor for the early diagnosis of sleeping sickness, *Phys.org.* Retrieved from: https://phys.org/news/2012-12-bioscientists-biosensor-early-diagnosis-sickness.html

[32] Rocha-Gaso, M,, Villarreal-Gómez, L., Beyssen, D., Sarry, F., Reyna, M. and Ibarra-Cerdeña, C., 2017. Biosensors to diagnose Chagas disease: A Brief Review, *Sensors.* **17(11)** 2629.

[33] Krampa. F., Aniweh, Y., Awandare, G. and Kanyong, P., 2017. Recent progress in the development of diagnostic tests for malaria, *Diagnostics*. **7(3)** 54.

[34] Walsh, J.E., Kavanagh, K.Y., Fennell, S., Murphy, J. and Harmey, M., 2000. Fibre optic micro-spectrometers for biomedical sensing, *Trans. Meas. Sci*. **22(5)** 355-369.

[35] Kavanagh, K.Y., Walsh, J.E., Murphy, J., Harmey, M., Farrell, M.A., Hardimann, O. and Perryman, R., 1999. Microspectrophotometric analysis of respiratory pigments using a novel fibre optic dip-probe in microsamples, *Physiol. Meas.* **20** 303-311.

[36] Bosschaart, N., Edelman, G.J., Aalders, M.C.G, van Leeuwen, T.G. and Faber, D.J., 2014. A literature review and novel theoretical approach on the optical properties of whole blood, *Lasers Med Sci.* **29(2)** 453-479.

[37] Takatani, S. and Graham, M.D., 1987. Theoretical analysis of diffuse reflectance from a two-layer tissue model, *IEEE Trans. Biomed. Eng.* **bme-26** 656-664.

[38] Prahl, S., 1999. Optical absorption of haemoglobin, *Tech. Rep., Oregon Medical Laser Center, Portland, Ore, USA.* Retrieved from: http://omlc.ogi.edu/spectra/hemoglobin/index.html

[39] Liu, P., Zhu, Z., Zeng, C. and Nie, G., 2012. Specific absorption spectra of hemoglobin at different PO2 levels: potential noninvasive method to detect PO2 in tissues, *J Biomed Opt.* **17(12)** 125002.

[40] Zijlstra, W.G., Buursma, A. and van Assendelft, O.W., 2000. *Visible and Near Infrared Absorption spectra of Human and Animal Haemoglobin*: *Determination and Application*, VSP International Science Publishers, Netherlands.

[41] Wimberley, P.D., Fogh-Andersen, N., Siggaard-Andersen, O., Lundsgaard, F. and Zijlstra, W.G., 1988. Effect of pH on the absorption spectrum of human oxyhemoglobin: a potential source of error in measuring the oxygen saturation of haemoglobin, *Clin Chem.* **34(4)** 750-4.

[42] Word Health Organization, 2016. *Malaria parasite counting malaria microscopy standard operating procedure,* MM-SOP-09. Retrieved from: http://www.wpro.who.int/mvp/lab_quality/2096_oms_gmp_sop_09_rev1.pdf

[43] Ghaffar, M.A., El-Melegy, M., Afifi, A.F., El Deen, B., El-Aswad, W., El-Kady, N. and Atia, A.F.I., 2016. The histopathological effects of Trypanosoma evansi onexperimentally infected mice, *Menoufia Med J.* **29(4)** 868-873.

[44] Chadalavada, S., 2018. Trypanosoma cruzi: pathogenesis, epidemiology, and recent developments in the potential treatment of Chagas' disease, *Microbewiki*. Retrieved from: https://microbewiki.kenyon.edu/index.php/Trypanosoma_cruzi:_pathogenesis,_epidemiology,_and_recent_developments_in_the_potential_treatment_of_Chagas%27_disease

[45] Zalloum, A., O'Mongain, E., Walsh, J.E., Danaher, S. and Stapleton, L., 1993. Dye Concentration Estimation by Remotely Sensed Spectral Radiometry, *International Journal of Remote Sensing.* **14(12)** 2285-2300.

[46] Danaher, S., O'Mongain, E. and Walsh, J.E., 1992, A New Cross-correlation Algorithm and the Detection of Rhodamine-B Dye in Sea Water, *International Journal of Remote Sensing.* **13(9)** 1743-1755.

Development of an Optical Biosensor for the Detection of *Trypanosoma evansi* and *Plasmodium berghei*

Hay Thi Theint[1], James Edward Walsh[2], Wong Siew Tung[1], Kenny Voon Gah Leong[1] and Mahendran Shitan[3]

[1]Pathology Department, International Medical University, Kuala Lumpur Malaysia
[2]Centre for Pre-University Studies, International Medical University, Kuala Lumpur Malaysia
[3]School of Mathematical and Computer Sciences, Heriot-Watt University, Putrajaya, Malaysia

A laboratory prototype system that correlates murine blood absorbance with degree of infection for *Plasmodium berghei* and *Trypanosoma avensi* has been designed, constructed and tested.

Spectral absorption results indicate a statistically relevant correlation at a 650 nm with infection for Plasmodium from between 4 and 7 sampling days' post infection, in spite of significant standard deviations among the sample populations for control and infected mice.

No significant spectral absorption change for Trypanosoma infection was been detected from the current data.

Corresponding stained slides of control and infected blood at each sampling date were taken with related infected cell counts determined and these correlate well for Plasmodium absorbance at 650 nm.